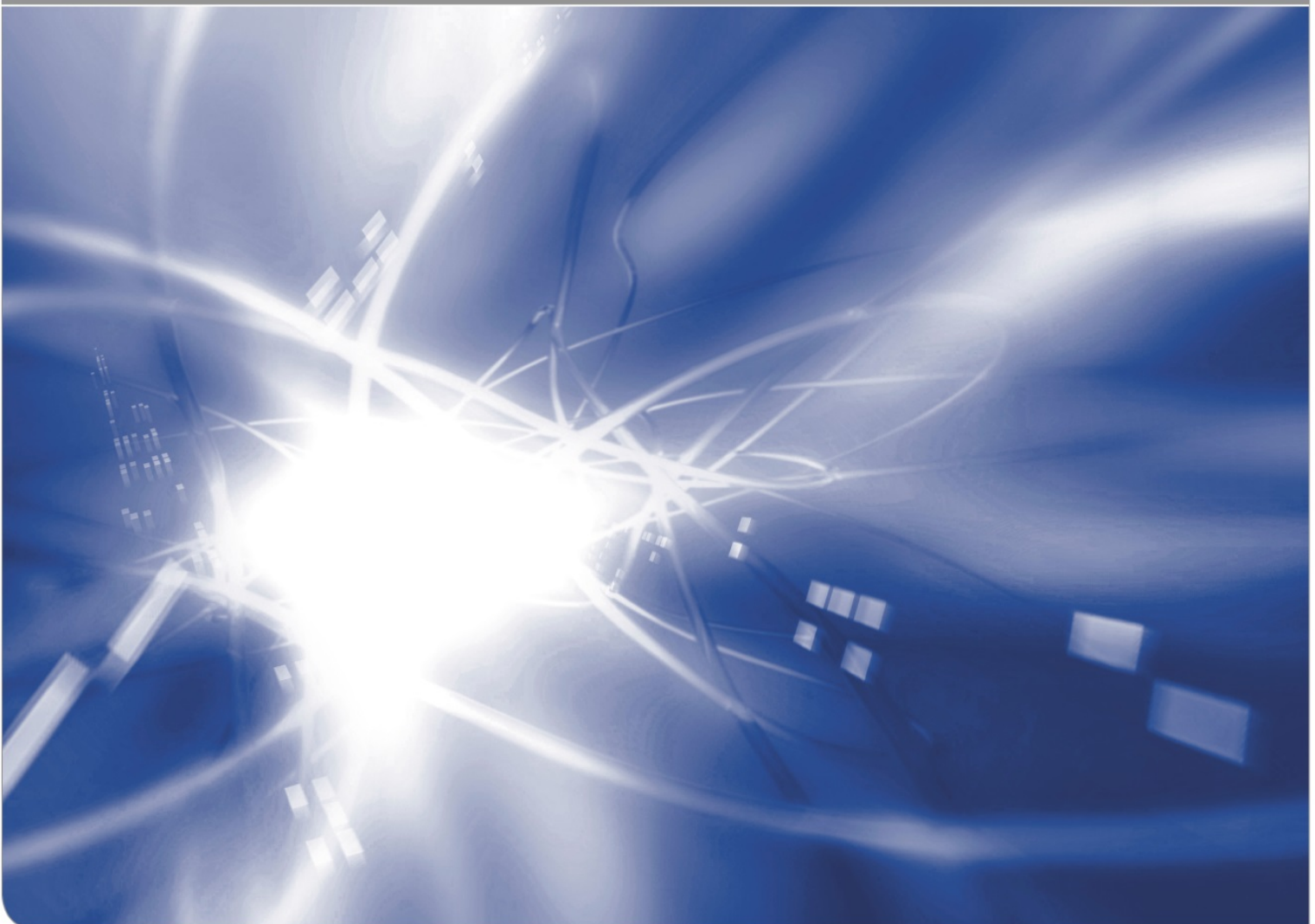


Mass transfer coefficients for water at silica surfaces

- Additional results

Günter Schell, Theo Fett

KIT SCIENTIFIC WORKING PAPERS 73



Institut für Angewandte Materialien, IAM
Karlsruher Institut für Technologie (KIT)

Impressum

Karlsruher Institut für Technologie (KIT)
www.kit.edu



This document is licensed under the Creative Commons Attribution – Share Alike 4.0 International License (CC BY-SA 4.0): <https://creativecommons.org/licenses/by-sa/4.0/deed.en>

2017

ISSN: 2194-1629

Abstract

Monotonously increasing water concentrations at silica surfaces can be described by a mass transfer surface condition for diffusion that hinders free water penetration from a water vapour environment into silica. So far, the related mass transfer coefficient has been determined predominantly from water uptake measurements. In this report, the data basis will be extended by taking into consideration further literature results on measurements of surface water concentrations and by evaluation of disk curvature measurements.

Contents

1	Determination of the mass transfer coefficient	1
2	Re-evaluation of data from literature	2
3	Mass transfer coefficients from disk curvature measurement	4
3.1	Swelling stresses in water-soaked silica disks	4
3.2	Hydroxyl concentration	5
4	Conclusions from disk measurement	8
	References	9

1 Determination of the mass transfer coefficient

At a silica surface exposed to a water vapour environment, there is a monotonously increasing water concentration observed [1], that can be described by a diffusion surface condition of

$$\frac{dC}{dz} = \frac{h}{D}(C - C_0) \quad \text{at } z=0, \quad (1.1)$$

where D is the water diffusivity, C_0 the asymptotically reached water concentration and a parameter h that describes reduced water entrance [2, 3]. Under this boundary condition the surface concentration at the surface reads as a function of time t [4]

$$C(0, t) / C_0 = 1 - \exp\left[\frac{h^2}{D}t\right] \operatorname{erfc}\left[h\sqrt{\frac{t}{D}}\right], \quad (1.2)$$

The molecular water uptake per surface unit, m_C , after time t results by integrating the water profile over the specimen thickness. As shown in [3] it results

$$m_C = \int_0^\infty C(z) dz = C_0 \frac{D}{h} \left\{ \frac{2}{\sqrt{\pi}} \frac{h}{\sqrt{D}} \sqrt{t} - \left(1 - \exp\left(\frac{h^2}{D}t\right) \operatorname{erfc}\left(h\sqrt{\frac{t}{D}}\right) \right) \right\} \quad (1.3)$$

For large values of $h\sqrt{(t/D_0)}$ the water uptake tends asymptotically to

$$m_\infty \rightarrow C_0 \left\{ \frac{2}{\sqrt{\pi}} \sqrt{tD} - \frac{D}{h} \right\} \quad (1.4)$$

Uptake measurements by Wakabayashi and Tomozawa [5] on Suprasil W, type-IV glass were used in [3] to determine the parameter h/\sqrt{D} by fitting eqs.(1.3) and (1.4) to the measurements. The fitted-parameters h/\sqrt{D} via eq.(1.3) are plotted in Fig. 1b as the open circles. An evaluation via eq.(1.4) resulted in the triangles.

The straight line in Fig. 1b representing open circles and triangles together reads

$$\frac{h}{\sqrt{D}} = A \exp\left(-\frac{Q}{RT}\right) \quad (1.5)$$

The fitting parameters are: $\log(A)=5.82$ [5.0, 6.64] for A in $(1/h^{1/2})$ and $Q=35.1$ [30.5, 39.7] (kJ/mol) with the 90% Confidence Intervals (CI) in brackets. Surface concentration values for molecular water obtained from measurements by Oehler and Tomozawa [1] (high purity silica glass made by CVD) are introduced in Fig. 1b as the solid circle. Surface water concentrations by Wakabayashi and Tomozawa [5] and Davis and Tomozawa [6] result in a clearly lower value (square). The 90% CI is given by the bars.

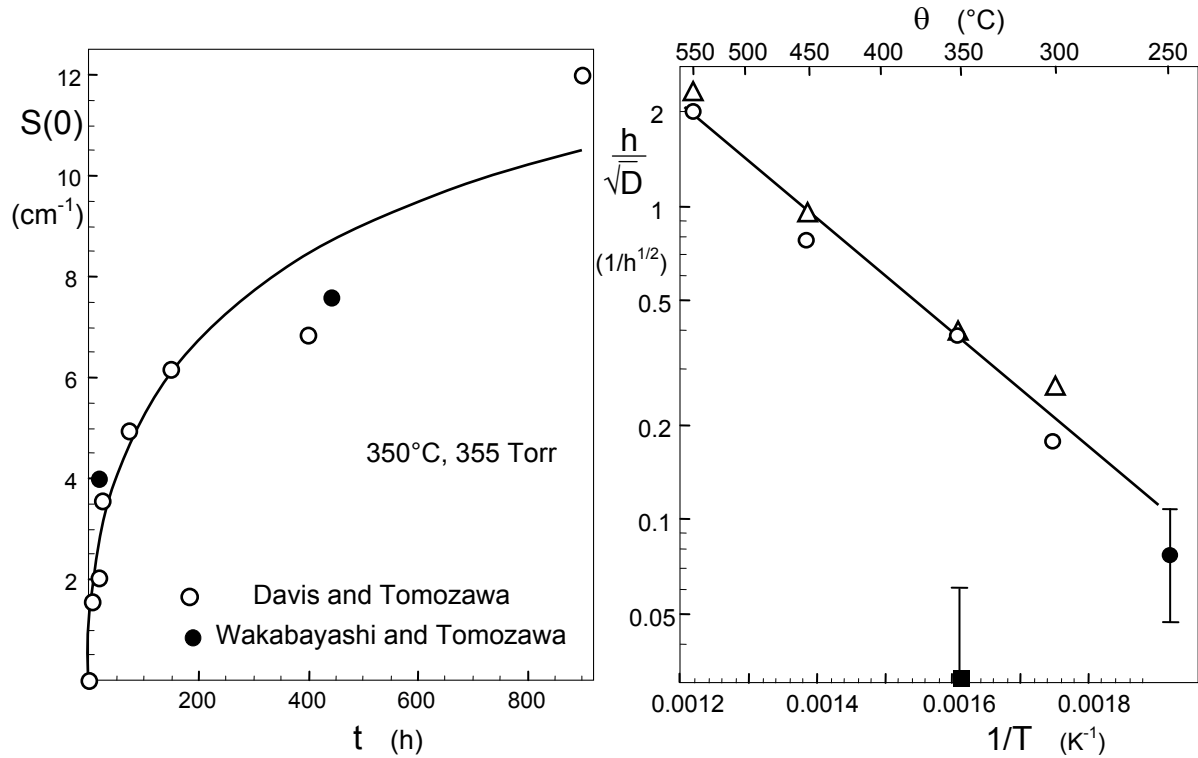


Fig. 1 Hydroxyl surface concentration after hydration at 350°C in water vapour at 355mm Hg; measurements were made by Wakabayashi and Tomozawa [5] (solid circles) and Davis and Tomozawa [6] (open circles), b) parameter h/\sqrt{D} as a function of temperature; circles: evaluation by fitting via eq.(1.3), triangles: results from the asymptotic behaviour via eq.(1.4). Solid circle represents data from Oehler and Tomozawa [1] at saturation pressure. Square gives a result from Fig. 1a by Wakabayashi and Tomozawa [5] and Davis and Tomozawa [6] for 355 Torr (ordinates scaled in terms of the IR absorption coefficient).

In context with the results from water uptake, it should be emphasized that the activation energy Q of eq.(1.5) is astonishingly close to half of the activation energy for the diffusivity that is given by Zouine et al. [8] as 72.3 ± 2 kJ/mol. From a numerical point of view this means roughly

$$\frac{h}{\sqrt{D}} \approx \text{const.} \times \sqrt{D_{\text{Zouine}}} \quad (1.6)$$

2 Re-evaluation of data from literature

Considering again the data in Fig. 1, large scatter in the measurements is noticeable and the deviations of the individual data points from the fitting curve are enormous. This holds especially for soaking times >400 h and is clearly caused by the high value at 900h, which appears extremely questionable.

Therefore, we excluded the 900h-value and fitted eq.(1.2) to the remaining data. The fit result was found as $h/\sqrt{D} = 0.11$ [0.077,0.148] ($1/\sqrt{h}$). The related curve is introduced in Fig. 2a as the solid line. The dashed curve represents again the result from Fig. 1a.

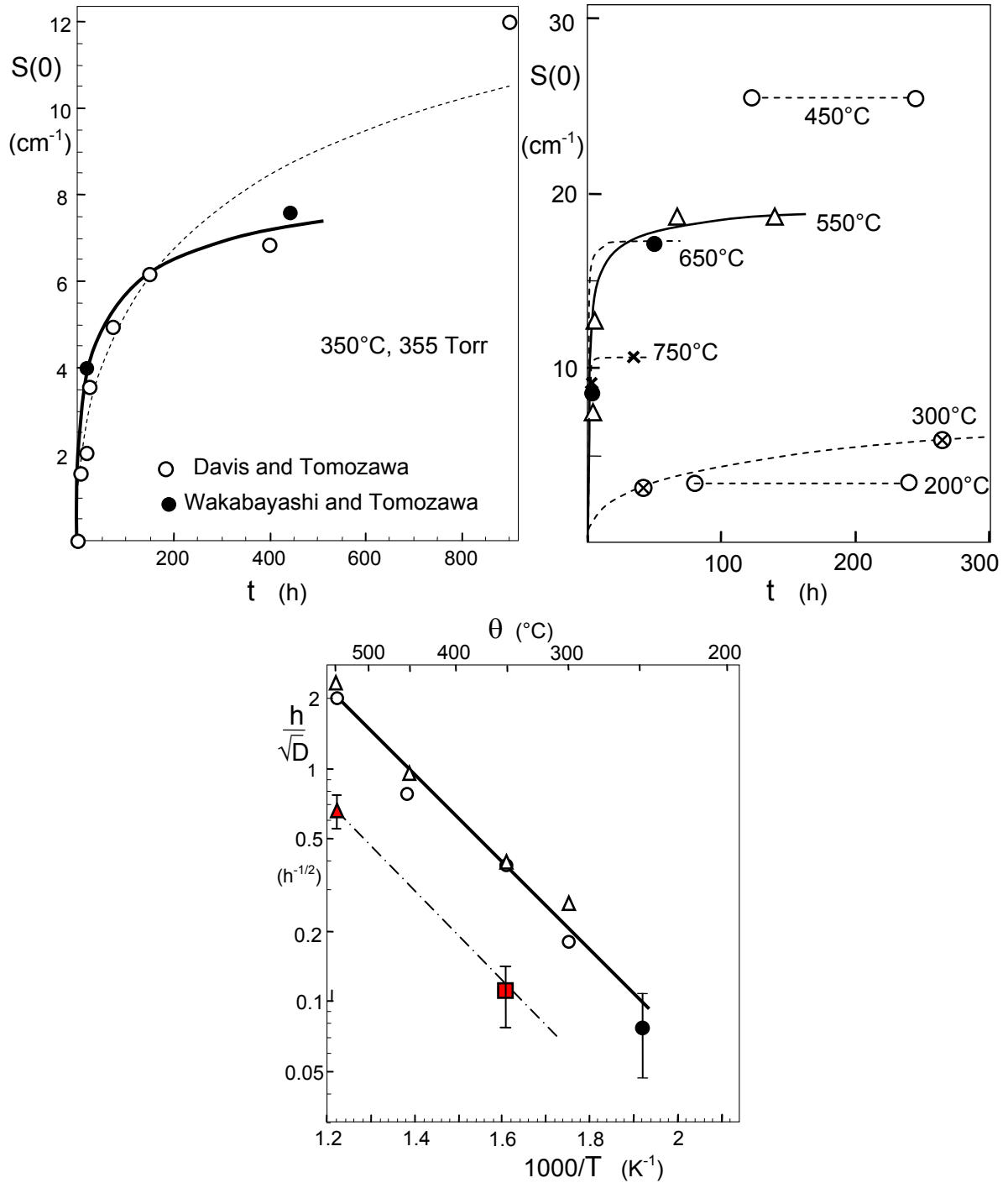


Fig. 2 a) Re-evaluation of strongly scattering data by Davis and Tomozawa [6] neglecting the data point at 900h, b) additional data by Wakabayashi and Tomozawa [5], c) parameters h/\sqrt{D} evaluated from Figs. 2a and 2b shown as red symbols.

In the paper by Wakabayashi and Tomozawa [5] additional data of surface concentrations are reported. These results were obtained by stepwise removal of the surface via etching. Figure 2b shows results for different temperatures. These data were fitted with eq.(1.2) yielding $h/\sqrt{D}=0.66$ [0.56, 0.75] ($1/\sqrt{h}$). For the other temperatures, only two

data points were available so that the application of a fitting procedure was not possible. Table 1 compiles the new results of Fig. 2c introduced by the red symbols.

Temperature (°C)	Basis data	h/\sqrt{D} ($1/\sqrt{h}$)	Surface concentration (cm^{-1})
350	[5,6]	0.11 [0.077,0.148]	9.4
550	[5]	0.66 [0.56, 0.75]	20.2

Table 1 Additional mass transfer coefficients from curve fitting via eq.(1.2).

3 Mass transfer coefficients from disk curvature measurement

3.1 Swelling stresses in water-soaked silica disks

The effect of the water-silica reaction is the generation of *swelling strains*. *Swelling stresses* are a consequence of the mechanical boundary conditions. A volume element in a thick plate that undergoes swelling cannot freely expand. If the diffusion zone is small compared to the component dimensions; expansion is completely prevented in the plane of the surface and can only take place normal to the surface plane.

At a free surface, the stress state is plane stress and, consequently, also stresses caused by swelling are equi-biaxial ($\sigma_x=0$)

$$\sigma_y = \sigma_x = -\frac{\varepsilon_v E}{3(1-\nu)} = -\frac{E}{3(1-\nu)} \kappa S \quad (3.1)$$

where $E=72$ GPa is Young's modulus and $\nu=0.17$ is Poisson's ratio. With these parameters, eq.(3.1) reads simply

$$\sigma_y = \sigma_x = -28\text{GPa} \times S \quad (3.2)$$

Swelling stresses were obtained in [7] for a GE-124 type-I glass by measuring the change of the curvature of silica disks after hot-water soaking. By measuring the radius of curvature at the surfaces of the curved disks and by understanding the mechanism of water migration, the surface stress can be calculated.

Figure 3 shows the surface stresses as a function of time. In context with the data scatter, it should be mentioned that the individual data points represent slightly different soaking temperatures.

Temperature/ Exposure Time	Surface stress (MPa)	h/\sqrt{t} ($1/\sqrt{h}$)	Diffusivity (cm^2/s)
196 °C/20h	-46.9 [45.9, 47.9]	0.111 [0.107, 0.115]	1.19×10^{-12}
216 °C/20h	-50.3 [49.7, 50.9]	0.0817 [0.080, 0.083]	1.97×10^{-12}
201 °C/96h	-54.7 [51.2, 58.3]	0.0575 [0.052, 0.064]	1.36×10^{-12}
188 °C/168h	-53.5 [52.0, 54.9]	0.0571 [0.054, 0.060]	0.64×10^{-12}

Table 2: Surface stresses, mass transfer parameter h/\sqrt{t} , and diffusivity, 90%-Confidence Intervals in brackets.

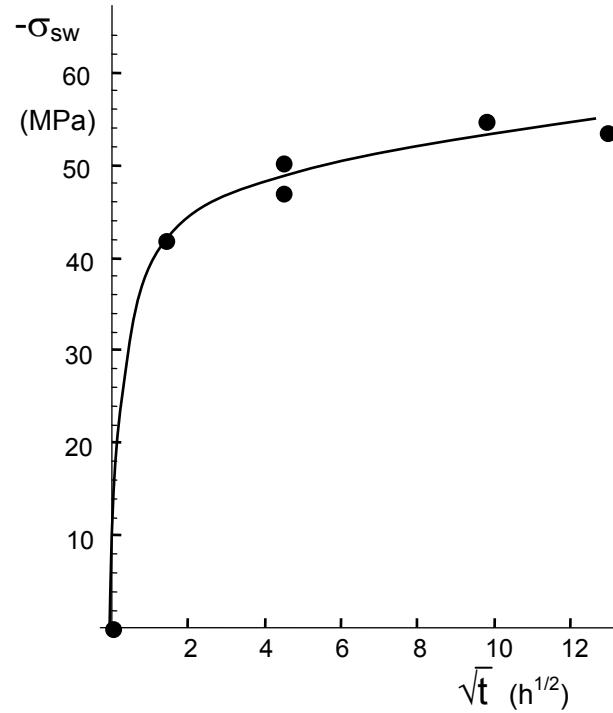


Fig. 3 Maximum swelling stresses, results from [7] for temperatures in the range of $188^{\circ}\text{C} \leq \theta \leq 216^{\circ}\text{C}$.

3.2 Hydroxyl concentration

Water concentrations under saturation pressure are available from the investigation by Zouine et al. [8]. The results are plotted in Fig. 4a and can be represented by

$$C_w = 0.000780 \exp(0.00868 \theta) \quad (3.3)$$

From these measurements, also the water species S and C can be obtained. In molar units, the total water concentration is given by

$$C_w = C + \frac{1}{2}S = C(1 + \frac{1}{2}k_1) \quad (3.4)$$

where the quantity k is the equilibrium constant. Equations (1.2) and (3.4)

$$S = \frac{C_w}{\left(\frac{1}{2} + \frac{1}{k_1}\right)} \quad (3.5)$$

and in *mass units*

$$S = \frac{17}{18} \frac{C_w}{\left(\frac{1}{2} + \frac{1}{k_1}\right)} \quad (3.6)$$

where the ratio 17/18 reflects the different mole masses of water and hydroxyl.

The equilibrium constant k_1 according to eq.(1.2) is obtained in [7] by an Arrhenius curve, that is expressed by

$$k_1 = 32.3 \exp\left(\frac{-10.8 \text{ kJ/mol}}{RT}\right) \quad (3.7)$$

where T is the absolute temperature, and R the gas constant.

Figure 4b gives the S -data in a plot with the temperature θ as the abscissa. The straight line introduced in this plot reads

$$S_{\text{sat}} = 0.000265 \exp(0.0143 \theta) \quad (3.8)$$

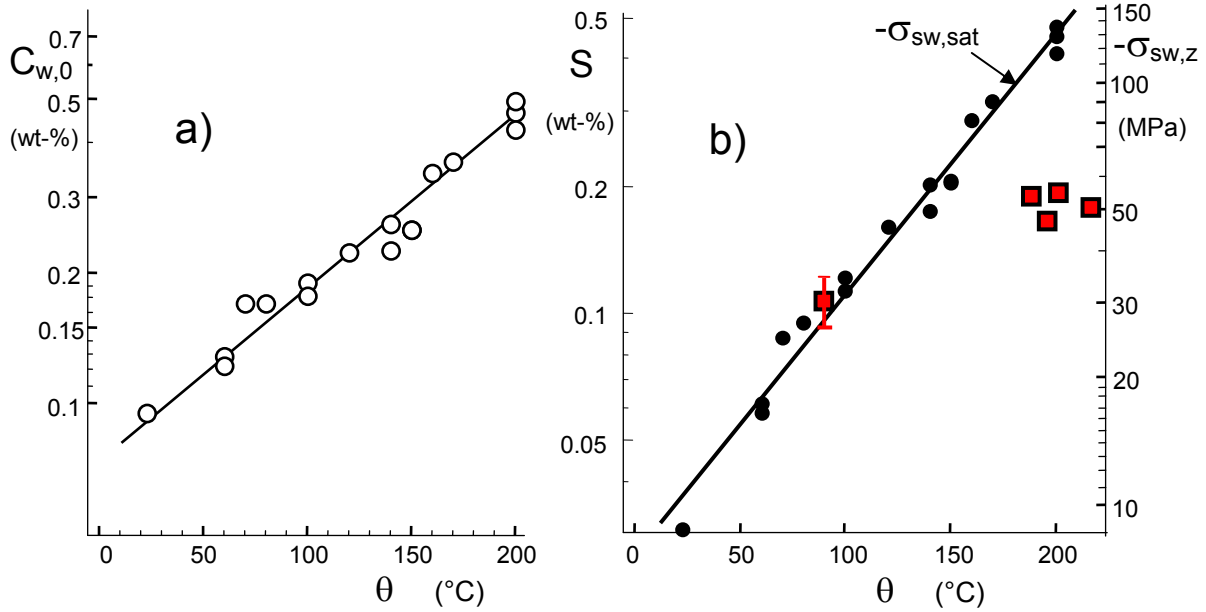


Fig. 4 a) Water concentration at silica surfaces under saturation pressure from measurements by Zouine et al. [8], solubility of hydroxyl water S , right ordinate: equi-biaxial swelling stresses, red squares: swelling stresses from disk experiments.

Introducing the hydroxyl concentrations from Fig. 4b into eq.(3.2) results in the equi-biaxial swelling stresses as is given by the right ordinate. The red squares in Fig. 4b represent the swelling stresses resulting from the disk experiments in [7]. At 90° the average value of $-31 \text{ MPa} \pm 1 \text{ SD} (\pm 4.2 \text{ MPa})$ is introduced. The agreement between predictions via eq.(3.2) and the measurements is good.

At 200°C the surface stress values of approximately -50 MPa deviate strongly from that for saturation conditions. Consequently, the water and hydroxyl concentrations are not yet in saturation.

Equation (1.2) allows determining the parameter h/\sqrt{D} from the stress measurements. Since the ratio of measured stresses and saturation stresses is known from Fig. 4b, we have to solve

$$1 - \exp\left[-\frac{h^2}{D}t\right] \operatorname{erfc}\left[h\sqrt{\frac{t}{D}}\right] = \frac{\sigma}{\sigma_{sat}} \quad (3.9)$$

The solutions were determined by application of the Mathematica Routine *FindRoot* [9]. The results can be introduced in Fig. 2b as plotted in Fig. 5 by the open squares. The values for the GE-124 type-I glass via deformation measurements are about 60% higher than the data given by eq.(1.5).

From the results of Fig. 5, we have to conclude that the parameter h/\sqrt{D} depends on the properties of the glass and probably on test conditions as water vapour pressure (in Fig. 5: saturation pressure and 355Torr water vapour pressure) and surface quality.

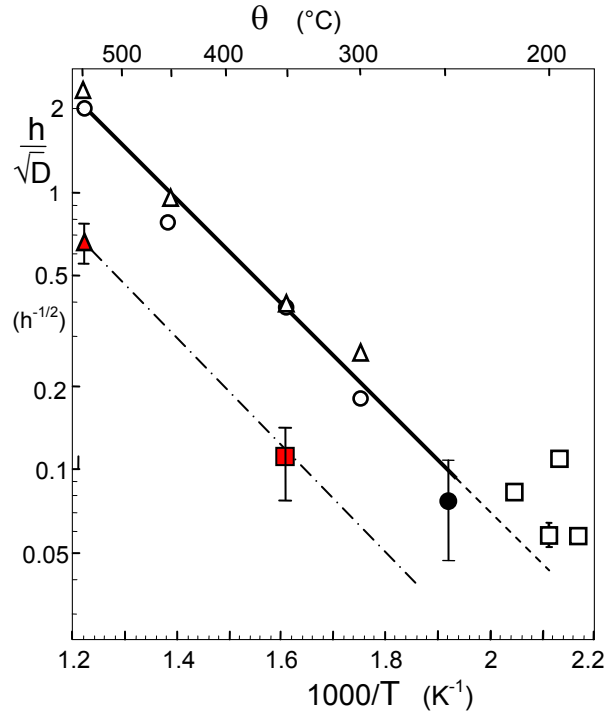


Fig. 5 Parameter h/\sqrt{D} as a function of temperature from [3], obtained from water uptake measurements by Wakabayashi and Tomozawa [5] (triangles and circles) on Suprasil W as a type-IV glass, Öhler and Tomozawa [1] (solid circle). Additionally plotted open squares: results from eq.(3.9) for the GE-124 glass.

Finally, Fig. 5 shows the diffusivities from for the GE-124 glass, Table 2 and [7], as the squares together with results by Zouine et al [8] for Infrasil 301 as the circles. The diffusivities from Table 2 exceed those from [8] by about 40%. However, they are still within the range of scattering.

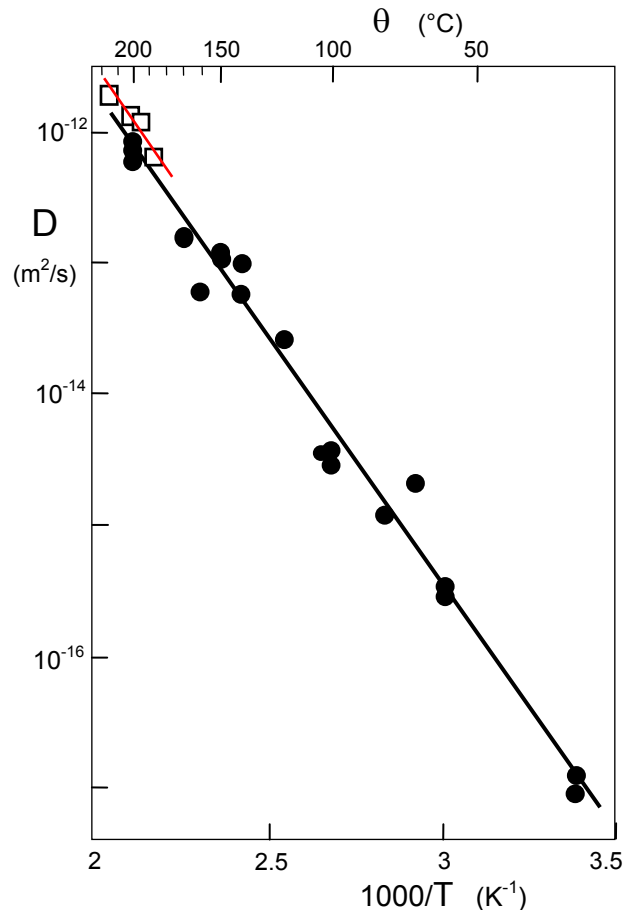


Fig. 6 Diffusivity as a function of temperature for silica glass Infracil 301 from [8] (circles), diffusivity for GE-124 glass from [7] (squares), see Table 2.

4 Conclusions from disk measurement

Both, heat transfer parameters from literature results on surface concentration measurements and disk curvature indicate scattering values for h/\sqrt{D} . Reasons may be the different silica qualities (type-I and -IV-glasses), vapour pressures (saturation pressure and 355Torr), and procedures (global water uptake and stepwise surface removal).

The parameters h/\sqrt{D} , determined by the disk-curvature measurements, are slightly higher than those from water uptake on the basis of results by Wakabayashi and Tomozawa [5]. In this context, a possible explanation may here be addressed:

The measurements of water uptake as a function of time were carried out in humid air with 355 Torr vapour pressure. In contrast, the disk curvatures were measured under saturation pressure of about 15 atm (1.55 MPa).

The diffusivity in the denominator of h/\sqrt{D} is affected by swelling as could be shown in [3]. The swelling stresses in the surface region must reduce the effective diffusivity.

This effect is stronger under saturation pressure since swelling stresses are proportional to the water concentration. Consequently, the parameter h/\sqrt{D} is higher for the disk measurements than for the uptake measurements at 355 Torr water vapour pressure.

References

- 1 Oehler, A., Tomozawa, M., Water diffusion into silica glass at a low temperature under high water vapor pressure, *J. Non-Cryst. Sol.* **347** (2004) 211-219
- 2 R.H. Doremus, *Diffusion of Reactive Molecules in Solids and Melts*, Wiley, 2002, New York.
- 3 S.M. Wiederhorn, G. Rizzi, S. Wagner, M.J. Hoffmann, T. Fett, Diffusion of water in silica glass in the absence of stresses, *J Am Ceram Soc.* **100** (2017), 3895–3902.
- 4 Carslaw, H.S., Jaeger, J.C. *Conduction of heat in solids*, 2nd ed. 1959, Oxford Press, London.
- 5 Wakabayashi, H., Tomozawa, M., Diffusion of water into silica glass at low temperature, *J. Am. Ceram. Soc.* **72** (1989), 1850-55.
- 6 Davis, K.M., Tomozawa, M., Water diffusion into silica glass: structural changes in silica glass and their effect on water solubility and diffusivity, *J. Non-Cryst. Sol.* **185** (1995), 203-220.
- 7 S. M. Wiederhorn, F. Yi, D. LaVan, T. Fett, M.J. Hoffmann, Volume Expansion caused by Water Penetration into Silica Glass, *J. Am. Ceram. Soc.* **98** (2015), 78-87.
- 8 A. Zouine, O. Dersch, G. Walter and F. Rauch, “Diffusivity and solubility of water in silica glass in the temperature range 23-200°C,” *Phys. Chem. Glass: Eur. J. Glass Sci and Tech. Pt. B*, **48** [2] (2007), 85-91.
- 9 *Mathematica*, Wolfram Research, Champaign, USA.

KIT Scientific Working Papers
ISSN 2194-1629

www.kit.edu